

Mass resolved angular distribution of fission fragments for near-barrier fusion-fission reactions

D. Vorkapić^{1,*} and B. Ivanišević²

¹Centre de Recherches Nucléaires, IN2P3-CNRS/Université Louis Pasteur, BP28, F-67037 Strasbourg Cedex, France

²Vinča Institute of Nuclear Sciences, P.O. Box 522, 11101 Belgrade, Yugoslavia

(Received 20 January 1997)

It is shown that K -equilibration fission can explain the decrease of mass resolved fission fragment anisotropy at larger mass asymmetries. Two competing mechanisms contribute to the anisotropy. The effective moment of inertia and K_0^2 decreases with the increase of mass asymmetry and contribute to the increase of anisotropy. On the other hand, for larger asymmetries, the barriers are higher and lifetimes are longer. Such systems are more K equilibrated and will have smaller anisotropy. [S0556-2813(97)03005-7]

PACS number(s): 25.70.Jj

Measured fission fragment anisotropies at near- and sub-barrier energies in a number of target-projectile systems [1,2] are anomalously large compared to the predictions based on the standard saddle-point statistical model [3]. In the standard saddle-point model (SPM) [3] fission fragments are assumed to be emitted along the direction of the nuclear symmetry axis at the fission saddle point, which is taken to be the transition-state configuration. For a compound state of angular momentum I , the z component (along the beam) M , and the projection of angular momentum on the nuclear symmetry axis K , the angular distribution of fission fragments is given by

$$W_{MK}^I(\Theta) = \frac{(2I+1)}{4\pi} |d_{MK}^I(\Theta)|^2.$$

Here Θ is the observation angle with respect to the beam axis in the center-of-mass frame. For spin-zero nuclei the spin projection M onto the beam axis is zero. The distribution of K values is estimated by using a constant temperature level density argument at the fission saddle point

$$\rho(K) = \frac{\exp(-K^2/2K_0^2)}{\sum \exp(-K^2/2K_0^2)},$$

where $K_0^2 = J_{\text{eff}} T / \hbar^2$ and $1/J_{\text{eff}} = 1/J_{\parallel} - 1/J_{\perp}$.

The angular anisotropy of fission fragments is defined as the ratio of the cross section at 180° (0°) to that at 90° . It is shown in Ref. [4] that anomalous fragment anisotropies appear only for systems with entrance-channel mass asymmetry $\alpha = (A_T - A_P)/(A_T + A_P)$ smaller than the Businaro-Gallone critical mass asymmetry α_{BG} . On the other hand, for the reactions where the entrance channel corresponds to the case $\alpha > \alpha_{BG}$, the measured anisotropies are found to be in agreement with the prediction of the standard theory [3]. It must be pointed out that anomalous anisotropy exists for the reaction $^{12}\text{C} + ^{236}\text{U}$, which is very close to the theoretically calculated Businaro-Gallone critical mass asymmetry point ($\alpha = 0.903$ and $\alpha_{BG} = 0.897$).

*Permanent address: Vinča Institute of Nuclear Sciences, Belgrade, Yugoslavia.

It has been proposed [5,6] that preequilibrium fission can give rise to a large anisotropy at sub-barrier energies. It was postulated that the emission of fission fragments not only came from the compound nucleus but also may take place after equilibration of all degrees of freedom except the K degree of freedom.

On the other hand, the second explanation is based on the measurement of the fission fragment angular distributions for the reaction $^{16}\text{O} + ^{238}\text{U}$ at near-barrier energies [7,8]. It was interpreted by Hinde *et al.* [7,8] that collisions with the tips of the deformed ^{238}U target nuclei lead to quasifission, while collisions with the sides result in fusion-fission.

The angular anisotropy of individual fission fragments has been measured by Cohen *et al.* [9] in 22 MeV proton-induced reactions of ^{232}Th , ^{235}U , ^{238}U , and ^{233}U . It was observed that asymmetric products have higher anisotropy than symmetric products. Similar observations were also found by Kudo *et al.* [10], Goswami *et al.* [11], Kapoor *et al.* [12], and Datta *et al.* [13]. All the measurements on proton and α -induced fission of actinide nuclei show an increase in anisotropy with an increasing mass asymmetry of fission fragments.

The mass resolved angular distributions of fission fragments have been measured by John *et al.* [14] in ^{10}B -, ^{12}C -, and ^{16}O -induced fission of ^{232}Th at near-barrier energies. The mass dependence of fragment anisotropy in the fission of $^{11}\text{B} + ^{237}\text{Np}$ and $^{16}\text{O} + ^{209}\text{Bi}$ have been measured by Pant *et al.* [15]. The $^{10}\text{B} + ^{232}\text{Th}$, $^{11}\text{B} + ^{237}\text{Np}$, and $^{12}\text{C} + ^{232}\text{Th}$ systems showed no mass dependence of anisotropy. On the other hand, it was observed in the reactions $^{16}\text{O} + ^{232}\text{Th}$ and $^{16}\text{O} + ^{209}\text{Bi}$ that asymmetric fission fragments have smaller anisotropy than symmetric fragments. This is a new effect which deserves to be explained.

For proton- and α -induced fission of actinide nuclei, anisotropy increases with the increasing mass asymmetry of fission fragments. This effect is easy to explain. The effective moment of inertia J_{eff} at the saddle point decreases with increase of the asymmetry of mass division. The $K_0^2 = J_{\text{eff}} T / \hbar^2$ decreases with the increase of asymmetry and therefore the angular anisotropy will increase for larger mass asymmetries. For the reactions where $\alpha < \alpha_{BG}$ ($^{16}\text{O} + ^{232}\text{Th}$) the pre-equilibrium fission is the dominant process and we expect explanations in the framework of the K -equilibration fission [KEF] model [5].

We will calculate the mass resolved angular distribution for the $^{16}\text{O} + ^{232}\text{Th}$ reaction at near-barrier energies. We have proposed that the K distribution is represented by a Gaussian around the most probable projection on the symmetry axis:

$$K_{\text{pro}} = I \sin \omega \cos \varphi,$$

where the initial orientation of the target is given by the angles ω and φ . The time-dependent variance $\sigma_K = ICt_m$ was used, where t_m is the mean of some time interval and C is a constant which represents the speed of K equilibration. The probability of fission was calculated for 18 different intervals of time. For each interval of time we have calculated the contribution of the angular distribution. The probability of fission for some time interval (τ_m, τ_{m+1}) is given by

$$P_m = \exp(-\tau_m/\tau_f) - \exp(-\tau_{m+1}/\tau_f),$$

where τ_f is the compound nucleus lifetime [16]. The compound nucleus lifetime is given by

$$\tau_f = \frac{h}{T[\exp(-B_f/T) - \exp(-E/T)]},$$

where B_f is the height of the fission barrier preventing the system from fast fission. In Ref. [5] we have calculated fission barriers B_f by the Sierk model [17] only for symmetric division. Here we have calculated fission barriers using the ‘‘funny hills’’ parametrization [18] both for symmetric and for different asymmetric divisions. The ‘‘funny-hill’’ barriers are higher than Sierk barriers. In order to reproduce the results of Ref. [5] we have compensated the increase of fission barriers by changing the parameter C (speed of K equilibration). Here we have used $C = 0.55 \times 10^{20} \text{ s}^{-1}$ instead of $C = 0.75 \times 10^{20} \text{ s}^{-1}$. We have calculated the mass resolved fission fragment angular distribution for the $^{16}\text{O} + ^{232}\text{Th}$ reaction at 92, 96, 100, and 85.7 MeV bombarding energies. Comparison of these calculations with experiment [14] are shown for 92, 96, and 100 MeV in Figs. 1(a), 1(b), and 1(c) respectively. The solid squares are experimental results [14] and the solid lines represent KEF model calculations. The experimental results show that anisotropy decreases with mass asymmetry of fission fragments at all three energies and this trend is theoretically reproduced. There is, however, sharp variation in anisotropy in the mass region 120–135 at all three energies.

For systems with $\alpha < \alpha_{BG}$, larger anisotropies for symmetric fragments as compared to asymmetric fragments can be explained taking into account the competition of two opposite effects. The first effect explains why anisotropy increases with mass asymmetry increase (as for p - and α -induced fission, where $\alpha > \alpha_{BG}$). The effective moment of inertia J_{eff} and K_0^2 decreases with an increase of asymmetry and this effect will contribute to the increase of anisotropy for larger mass asymmetries.

The second effect is connected to the K equilibration and fission barriers. For larger asymmetries the barriers are higher. According to Bohr [16], the compound nucleus life-

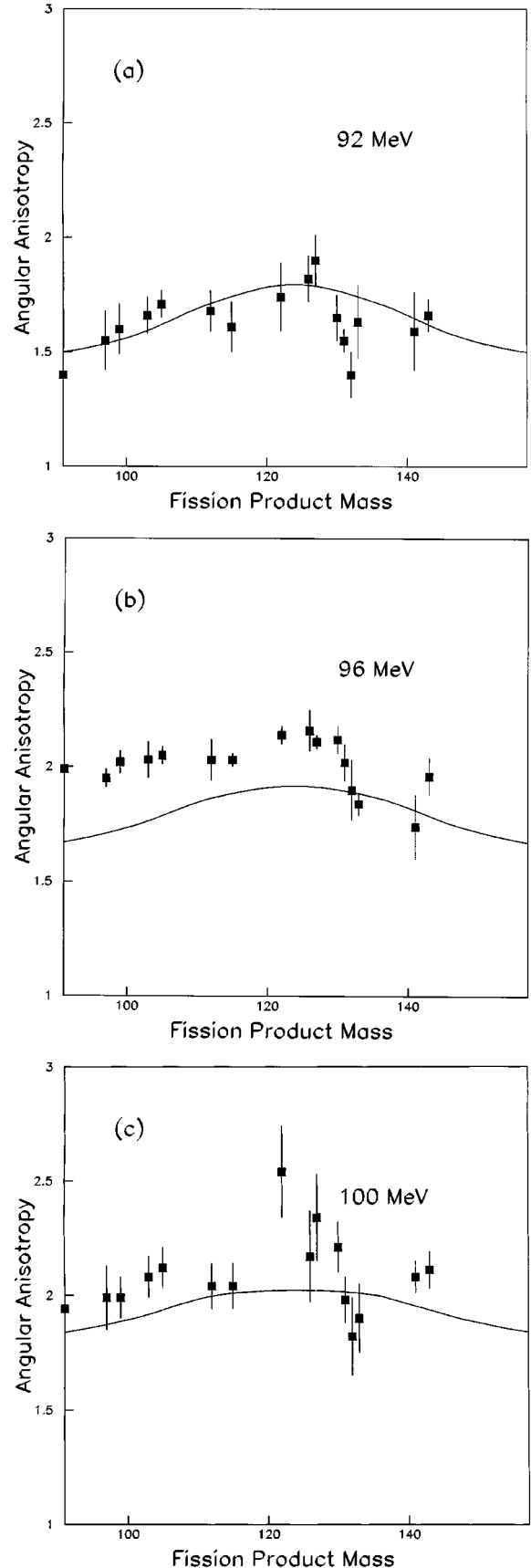


FIG. 1. Fission fragment angular anisotropy versus fission product mass for the $^{16}\text{O} + ^{232}\text{Th}$ reaction at $E_{\text{lab}} = 100, 96,$ and 92 MeV . The solid squares are experimental results and the solid lines present results of our theory.

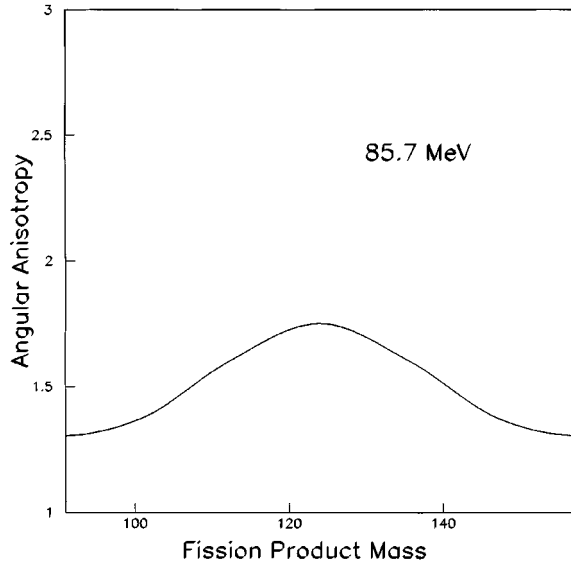


FIG. 2. Fission fragment angular anisotropy versus fission product mass for the $^{16}\text{O}+^{232}\text{Th}$ reaction at $E_{\text{lab}}=85.7$ MeV. The solid line presents results of our theory.

time τ_f is proportional to $\exp(B_f/T)$, that is, the lifetime of the system is longer for higher barriers (larger asymmetries). The system with longer lifetime will be more equilibrated and therefore will have smaller anisotropy. The second effect contributes to the decrease of anisotropy for larger mass asymmetries. From Figs. 1(a), 1(b), and 1(c) we see that the contribution of the second effect is stronger than the contribution of the first effect. In Fig. 2 we show expectations based on the KEF model for lower energies (for the $^{16}\text{O}+^{232}\text{Th}$ reaction at 85.7 MeV laboratory energy). This shows that the decrease of anisotropy is larger for asymmetric fragments at lower energies. We expect that contribution of the second effect will be even stronger for lower energies.

The importance of the deformation of the target is shown in Fig. 3. The solid lines present results of our theory for the deformed target, while the dashed lines present results for the target without deformation. The anisotropy difference between the results with the deformed target and with the target without deformation becomes larger at lower energies. The ratio of transmission coefficients for target orientation angles around 180° in comparison with angles around 90° will increase with a decrease of energy. For higher energies this ratio becomes equal to 1 and the difference between the two cases (with and without deformation) will disappear. Even in the case of the target without deformation, the decrease of anisotropy for asymmetric fragments compared to the anisotropy for symmetric fragments is larger for lower energies. The importance of angular momenta for this phenomena can be explained as follows. The fission barriers are lower for larger angular momenta. The difference between fission barriers for asymmetric and symmetric division $B_f(\text{asym})-B_f(\text{sym})$ is larger for lower angular momenta and the ratio of lifetimes for asymmetric and symmetric mass division is exponentially proportional to this difference:

$$\frac{\tau_f(\text{asym})}{\tau_f(\text{sym})} \sim \exp\left(\frac{B_f(\text{asym})-B_f(\text{sym})}{T}\right).$$

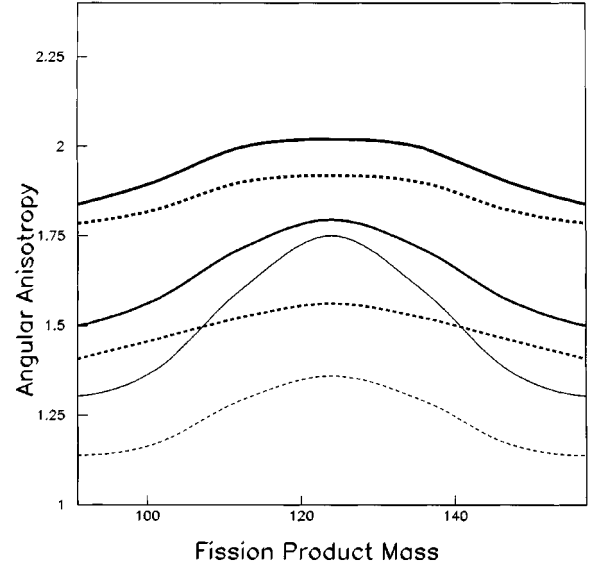


FIG. 3. Fission fragment angular anisotropy versus fission product mass for the $^{16}\text{O}+^{232}\text{Th}$ reaction at $E_{\text{lab}}=85.7, 92,$ and 100 MeV. The solid lines present the results of our theory with deformation of the target and dashed lines present the results of our theory without deformation. The two lines with the largest width represent the reaction at the energy of 100 MeV. The two lines of the medium width represent the reaction at 92 MeV, and the two lines of the smallest width represent the reaction at 85.7 MeV.

Therefore for lower angular momenta and lower energies the difference of angular anisotropy at the symmetric and asymmetric division is larger. The dashed lines in Fig. 3, which present the results without deformation, show that just this anisotropy difference becomes larger for lower energies.

In order to show the importance of the angular momentum for angular anisotropy we have calculated the angular anisotropy for the $^{16}\text{O}+^{232}\text{Th}$ reaction at 96 MeV laboratory

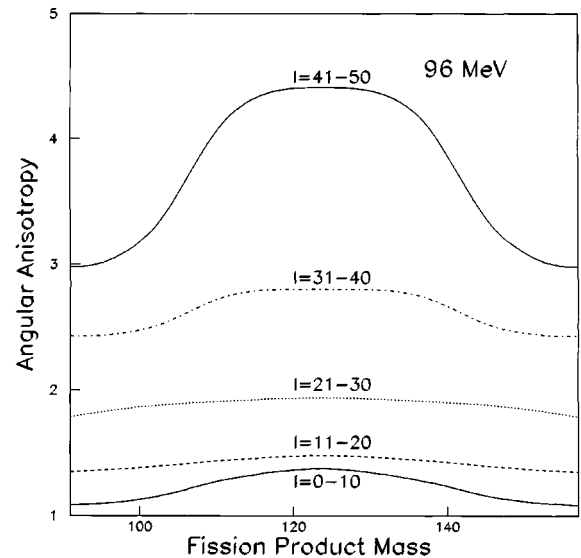


FIG. 4. Fission fragment angular anisotropy versus fission product mass for the $^{16}\text{O}+^{232}\text{Th}$ reaction at 96 MeV laboratory energy. Different lines show results of our theory for different angular momentum windows.

energy for different angular momentum windows ($I=0-10$, $11-20$, $21-30$, $31-40$, and $41-50$). These results are shown in Fig. 4. The anisotropy is larger for larger angular momenta due to lower barriers for higher angular momenta. The second and third angular momentum windows have a smaller difference in anisotropies for symmetric and asymmetric division in comparison to the first angular momentum window. This is already explained in Fig. 3. For larger angular momenta (fourth and fifth window) the difference of anisotropy for symmetric and asymmetric division again increases. For lower angular momenta for this reaction at 96 MeV laboratory energy the transmission coefficients are nearly equal for all orientations of the target. But, for larger angular momenta the transmission coefficients are larger for target orientation angles around 180° in comparison with angles around 90° and this explains the large difference for the fifth window of angular momenta.

Recently, fission fragment angular distributions have been measured [19,20] for ^{11}B , ^{12}C , ^{16}O , and $^{19}\text{F}+^{232}\text{Th}$ systems at sub-barrier energies. The mass averaged fission fragment anisotropy was found to exhibit an anomalous peaklike structure below the fusion barrier in all the measured systems. The decrease of angular anisotropy at deep sub-barrier energies cannot be explained by the model, which takes into

account only symmetric division. It may be that at deep sub-barrier energies, where the excitation energy is below 30 MeV, there is a significant increase of the asymmetric yield. It is shown in Fig. 1 that the mass resolved fission fragment anisotropy decreases as the asymmetry of fission increases. For low energy this decrease becomes significant (Fig. 2). Therefore, as the excitation energy decreases, the asymmetric yield increases, leading to decrease of mass averaged anisotropy.

In conclusion, mass resolved fission fragment angular anisotropies have been explained in the framework of the K -equilibration fission model. We have interpreted the results in terms of two competing mechanisms. The first mechanism explains why anisotropy increases with mass asymmetry increase for $\alpha > \alpha_{BG}$. The effective moment of inertia and K_0^2 decreases with an increase of mass asymmetry and contribute to the increase of anisotropy. The second mechanism is connected to K equilibration. For larger mass asymmetries the barriers are higher and the lifetime of the system is longer. Such systems will be more equilibrated and, therefore, will have smaller anisotropies.

One of us (D.V.) would like to thank Dr. G. Rudolf and the Demon group for discussion and kind hospitality, and also the French government for financial support.

-
- [1] R. Vandenbosch, J. Murakami, C.-C. Sahm, D. D. Leach, A. Ray, and M. J. Murphy, *Phys. Rev. Lett.* **56**, 1234 (1986).
- [2] T. Murakami, C.-C. Sahm, R. Vandenbosch, D. D. Leach, A. Ray, and M. J. Murphy, *Phys. Rev. C* **34**, 1353 (1986).
- [3] I. Halpern and V. M. Strutinsky, in *Proceedings of the Second United Nations International Conference on the Peaceful Uses of Atomic Energy*, Geneva, 1958 (United Nations, New York, 1958), Vol. 15, p. 408.
- [4] V. S. Ramamurthy *et al.*, *Phys. Rev. Lett.* **65**, 25 (1990).
- [5] D. Vorkapić and B. Ivanišević, *Phys. Rev. C* **52**, 1980 (1995).
- [6] Z. H. Liu, H. Q. Zhang, J. C. Xu, Y. Qiao, X. Qian, and C. J. Lin, *Phys. Lett. B* **353**, 173 (1995).
- [7] D. J. Hinde, M. Dasgupta, J. R. Leigh, J. P. Lestone, J. C. Mein, C. R. Morton, J. O. Newton, and H. Timmers, *Phys. Rev. Lett.* **74**, 1295 (1995).
- [8] D. J. Hinde, M. Dasgupta, J. R. Leigh, J. C. Mein, C. R. Morton, J. O. Newton, and H. Timmers, *Phys. Rev. C* **53**, 1290 (1996).
- [9] B. L. Cohen, B. L. Ferrel-Bryan, D. J. Coombe, and M. K. Hullings, *Phys. Rev.* **98**, 685 (1955).
- [10] H. Kudo, Y. Nagame, H. Nakahara, K. Miyano, and I. Kohno, *Phys. Rev. C* **25**, 909 (1982).
- [11] A. Goswami, S. B. Manohar, S. K. Das, A. V. R. Reddy, B. S. Tomar, and S. Prakash, *Z. Phys. A* **342**, 299 (1992).
- [12] S. S. Kapoor, D. M. Nadkarni, R. Ramanna, and P. N. Rama Rao, *Phys. Rev.* **137**, B511 (1965).
- [13] T. Datta, S. P. Dange, H. Naik, and S. B. Manohar, *Phys. Rev. C* **48**, 221 (1993).
- [14] B. John, A. Nijasure, S. K. Kataria, A. Goswami, B. S. Tomar, A. V. R. Reddy, and S. B. Manohar, *Phys. Rev. C* **51**, 165 (1995).
- [15] L. M. Pant, A. Saxena, R. K. Choudhury, and D. M. Nadkarni, *Phys. Rev. C* **54**, 2037 (1996).
- [16] N. Bohr and J. A. Wheeler, *Phys. Rev.* **56**, 426 (1939).
- [17] A. Sierk, *Phys. Rev. C* **33**, 2039 (1986).
- [18] M. Brack, J. Damgaard, A. S. Jensen, H. C. Pauli, V. M. Strutinsky, and C. Y. Wong, *Rev. Mod. Phys.* **44**, 320 (1972).
- [19] N. Majumdar, P. Bhattacharya, D. C. Biswas, R. K. Choudhury, D. M. Nadkarni, and A. Saxena, *Phys. Rev. C* **53**, R544 (1996).
- [20] N. Majumdar, P. Bhattacharya, D. C. Biswas, R. K. Choudhury, D. M. Nadkarni, and A. Saxena, *Phys. Rev. Lett.* **77**, 5027 (1996).